

INTRODUCTION

Tsunamis have a long history of devastation costing the lives of thousands of people, causing damage to property and infrastructures. To name a few of them, the deadliest 2004 Sumatra earthquake and tsunami, 2011 Tohoku Oki, and more recently, the 2018 Sulawesi and Palu tsunami. It implies the necessity of having a reliable early warning system (Williams et al 2021).

Current warning systems rely heavily on the Deep-ocean Assessment & Reporting of Tsunamis (DART network) for tsunami waves and seismic measurements for rupture detection, each within a separate early warning system. Accurate tsunami evaluation from DART buoys may be possible, though depending on particular circumstances (far distance generated tsunamis) there may not be sufficient time for early warning. On the other hand, seismic data provide valuable information on the tectonic movements, earthquake size, and possible epicenter, though with current technology and analysis they fail to assess the tsunami threat. Recently, Acoustic Gravity Waves (AGW), as another precursor of tsunami waves have been considered for the early detection of hazards (Abdolali et. al 2018; Gomez and Kadri 2021a). These waves are generated and propagated due to the slight compressibility of the water. AGWs radiate from submarine earthquakes alongside tsunamis and propagate through the liquid or elastic layers. They carry information about the source at relatively high speeds ranging from the speed of sound in water (1500m/s), to Rayleigh waves speed in the solid (3200 m/s) that far exceeds the phase speed of the tsunami (200m/s) at 4 km water depth while compression P (pressure) waves and S (shear) waves propagate at about 6,800 m/s and 3,900 m/s in the solid earth, respectively. The combined effect of water compressibility coupled to elastic earth also improved the accuracy of the numerical models for the prediction of surface gravity waves (Abdolali et. al 2019).

[VIDEO] https://res.cloudinary.com/amuze-interactive/video/upload/vc_auto/v1638894856/agu-fm2021/DE-FD-AB-DB-31-AC-5D-89-D9-1B-9B-1C-34-A7-8C-5A/Video/schamtic_trimmed_veldpc.mp4

Video 1- Surface Gravity (tsunami) and acoustics generation and propagation under the incompressible ocean-rigid bottom (upper panel), compressible ocean- rigid bottom (middle panel), and compressible ocean - elastic bottom (lower panel) assumptions.

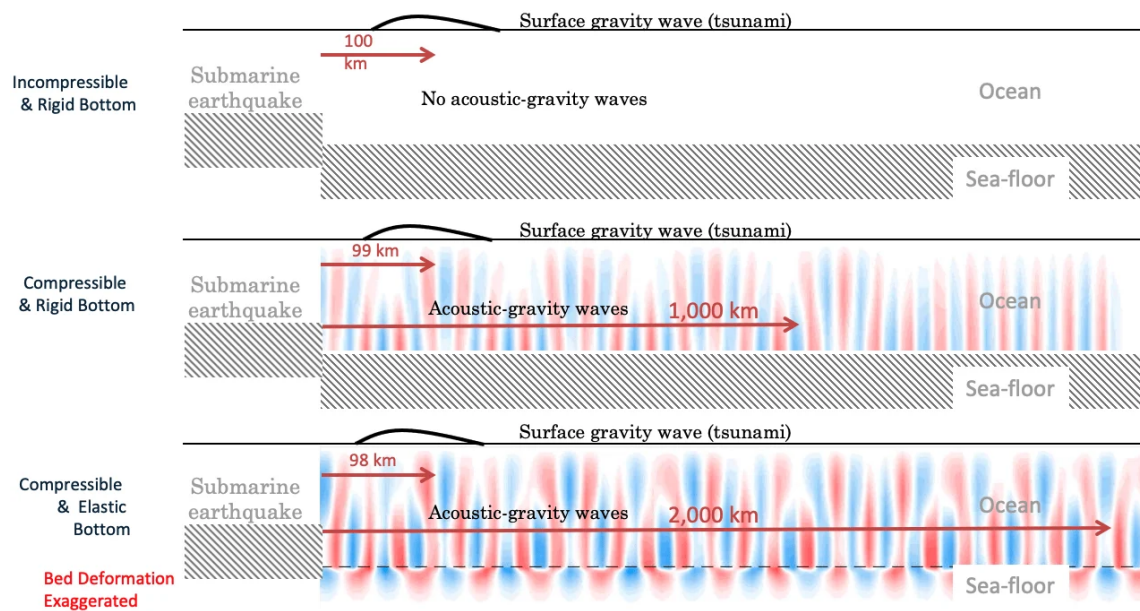


Figure 1- Surface Gravity (tsunami) and acoustics generation and propagation under the incompressible ocean-rigid bottom (upper panel), compressible ocean-rigid bottom (middle panel), and compressible ocean - elastic bottom (lower panel) assumptions.

SHORTEST PATH, TRAVEL TIME, INVERSE PROBLEM AND MACHINE LEARNING

The Dijkstra's algorithm is employed to find the shortest paths between the epicenter and all the wet nodes on a global triangular unstructured mesh using the phase speed of surface gravity waves, progressive acoustic modes within the water body, and P and S waves throughout earth. The phase speed estimator takes into account the simultaneous effects of the slight compressibility of water, sea-bed elasticity, and static compression of the ocean under gravity, leading to the precise calculation of the arrival time (Abdolali et. al 2019).

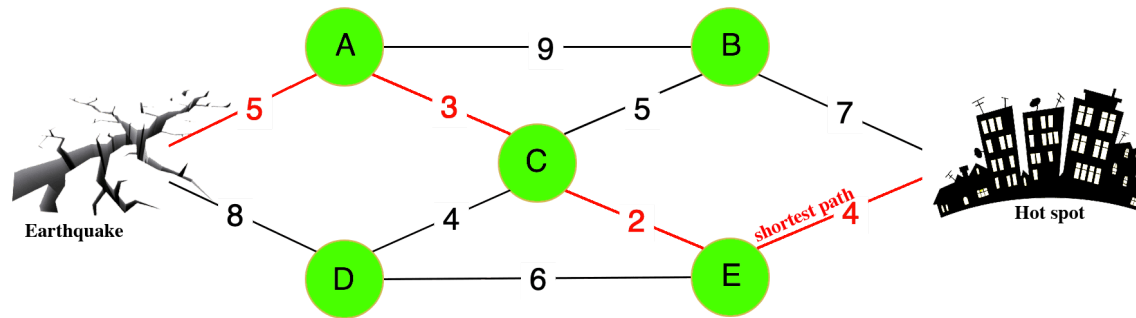
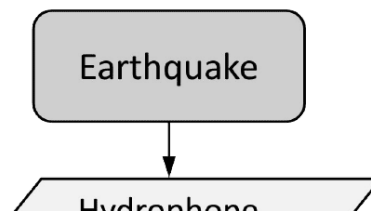


Figure 2- Schematic view of travel time calculation via Dijkstra's algorithm fastest/shortest path.

Employing digital signal processing techniques (DPS) we can analyze sound recordings of underwater earthquakes, that train artificial intelligence (AI) algorithms to classify the type of earthquake (i.e. horizontal or vertical) and its moment magnitude (strength) (Gomez and Kadri 2021b). This is a significant step for a reliable early tsunami warning system since the type of earthquake can dictate if a tsunami will be generated at all. For example, a more horizontal type movement will not generate a tsunami even if the magnitude of the earthquake is relatively large, but the vertical element has a direct relation. Moreover, AI algorithms were coupled with our semi-analytical inverse model (Gomez and Kadri 2021a) that calculates the dynamics and geometry of the fault, which in turn can give an estimation of the size of the generated tsunami.



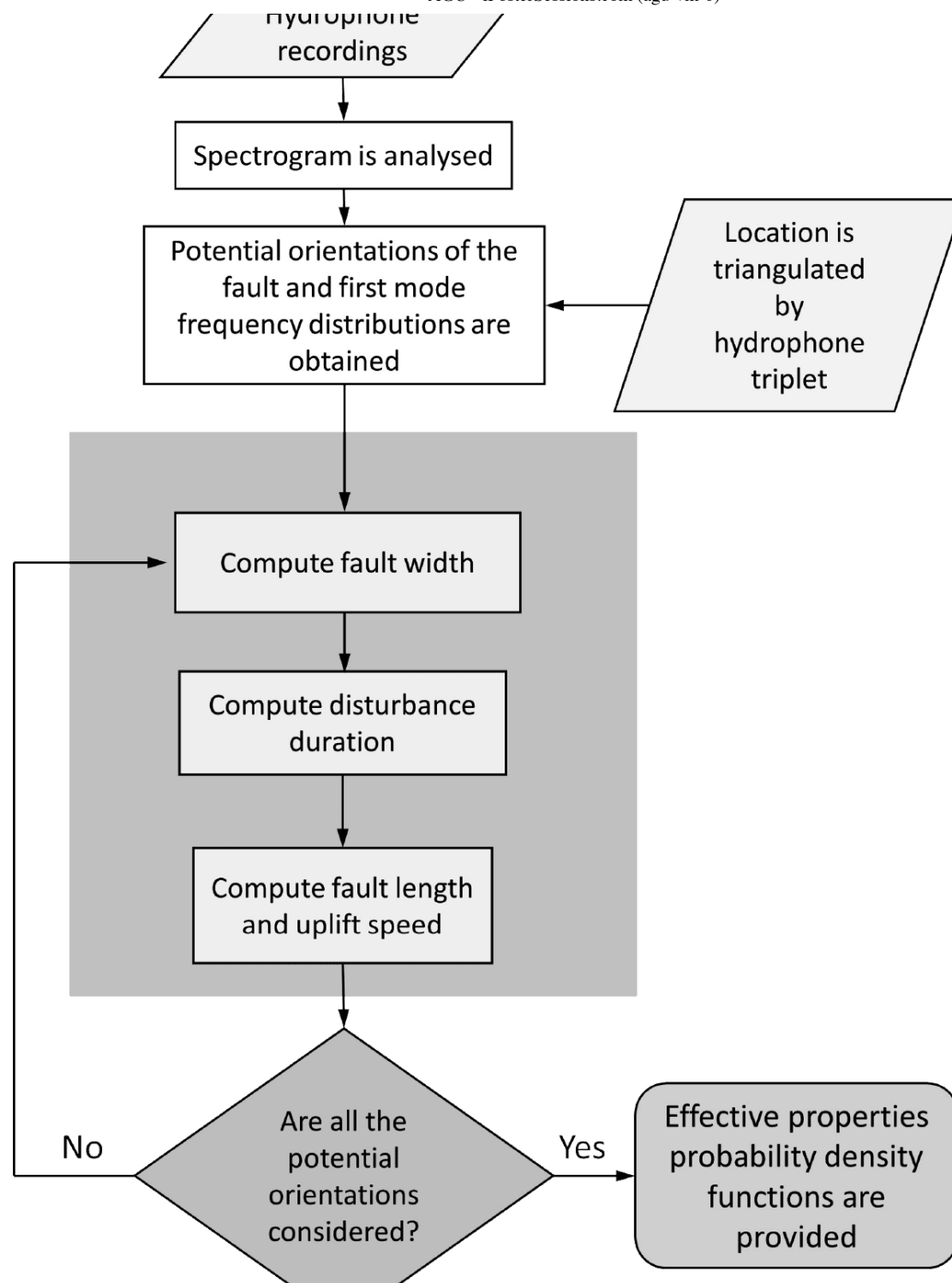


Figure 3- Inverse problem model process (Gomez and Kadri 2021b)

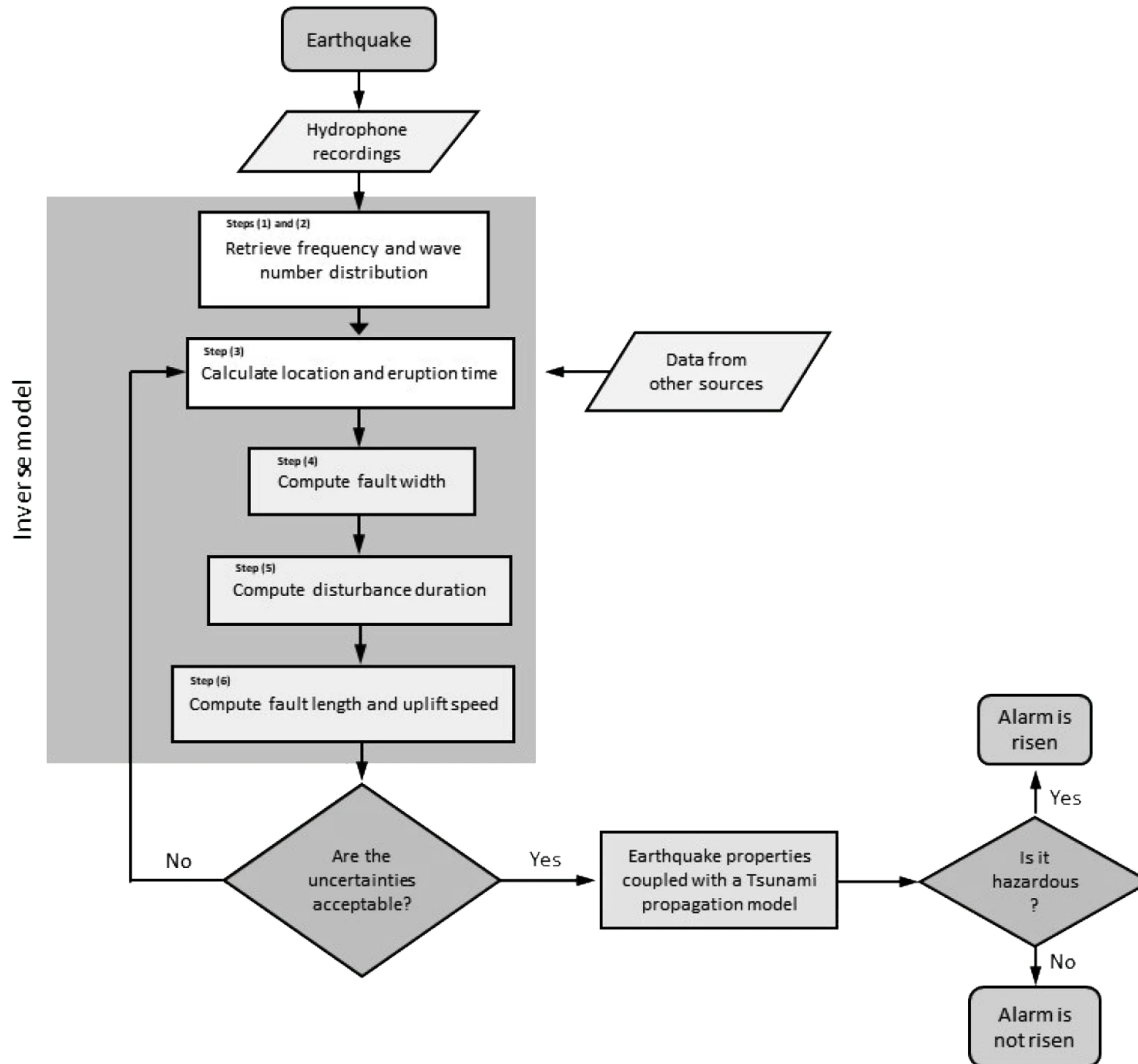


Figure 4- Inverse model application flowchart - from acoustic pressure signal arrival to probabilistic calculation of source properties (Gomez and Kadri 2021a).

EARLY WARNING END-TO-END WORKFLOW

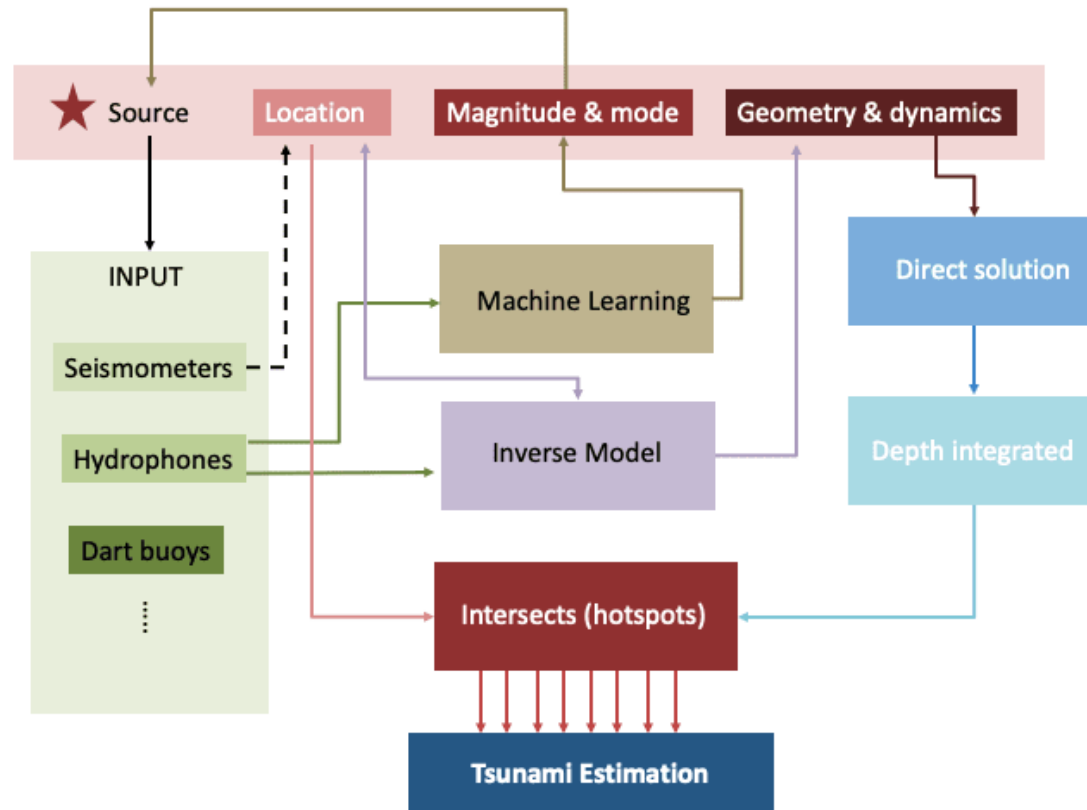


Figure 5 - Tsunami Early Detection workflow

[VIDEO] https://res.cloudinary.com/amuze-interactive/video/upload/vc_auto/v1638893223/agu-fm2021/DE-FD-AB-DB-31-AC-5D-89-D9-1B-9B-1C-34-A7-8C-5A/Video/inverse_trimmed_g7rjlb.mp4

Video 2- Probability density functions for the effective slender fault characteristics calculated by the inverse problem model for 21st December 2010 (27.10N, 143.76E) earthquake.

INCORPORATING WATER COMPRESSIBILITY AND EARTH ELASTICITY

[VIDEO] https://res.cloudinary.com/amuze-interactive/video/upload/vc_auto/v1639160562/agu-fm2021/DE-FD-AB-DB-31-AC-5D-89-D9-1B-9B-1C-34-A7-8C-5A/Video/prop_a1an0b.mp4

Video 3- Propagation of P, S, 3 acoustic model and surface gravity (tsunami) waves for 21st December 2010 (27.10N, 143.76E) earthquake.

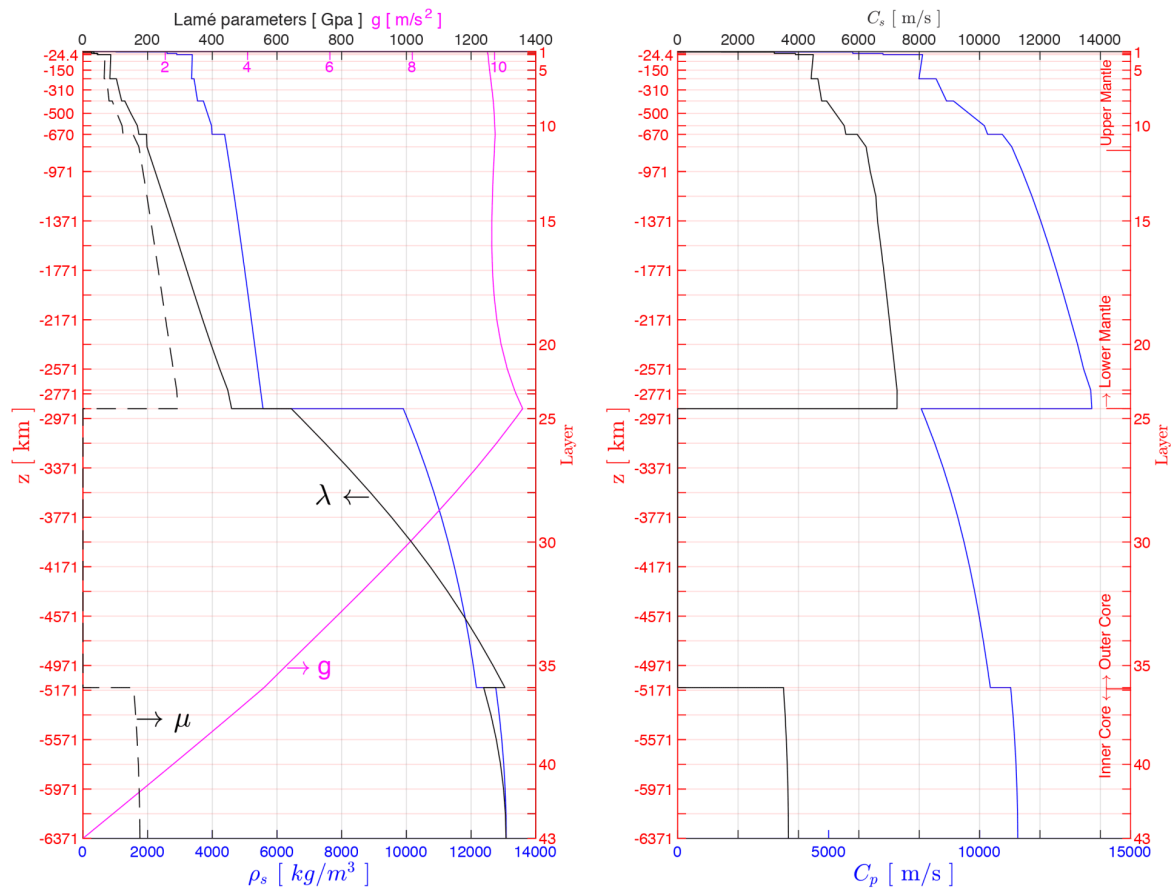


Figure 6 - PREM model profile (Dziewonski 1981). Left panel: Lamé constant profile, density and gravity (g); Right panel: Compressional wave speed (V_p) and shear wave speed (V_s).

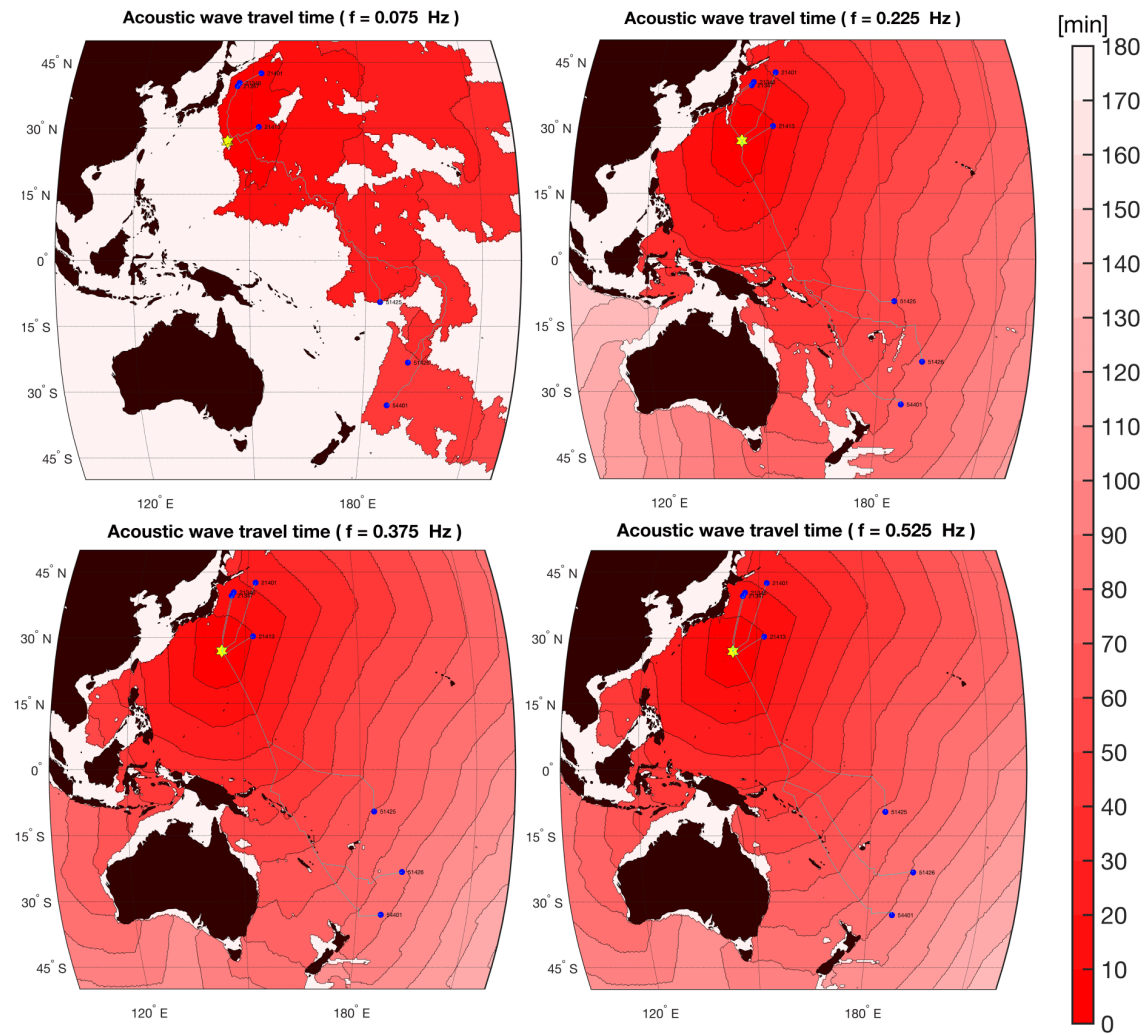


Figure 8- The first 4 dominant acoustic modes (governed by fault depth) Travel time for 21st December 2010 (27.10N, 143.76E) earthquake.

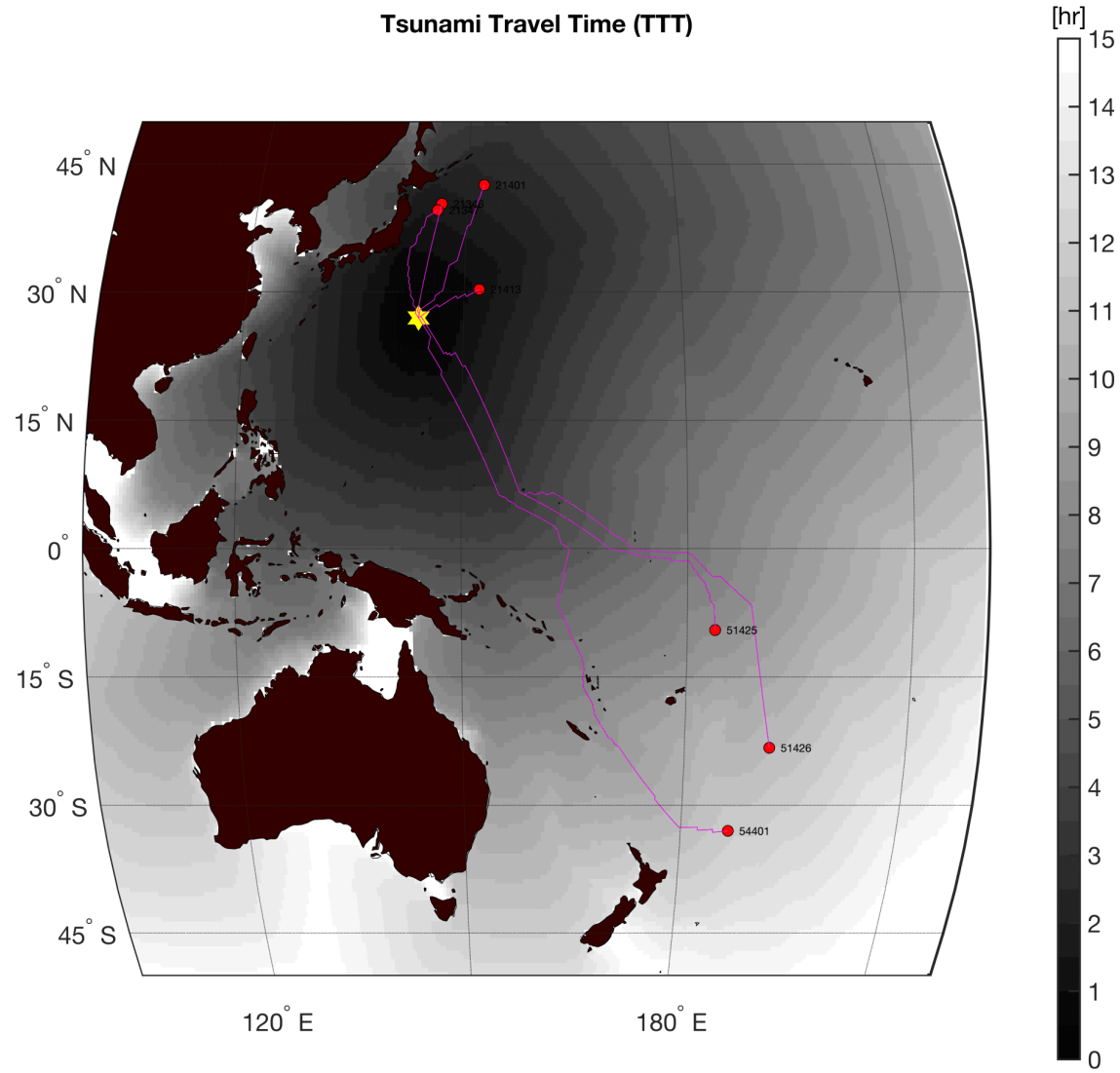


Figure 9- The surface gravity wave (tsunami) Travel time for 21st December 2010 (27.10N, 143.76E) earthquake.

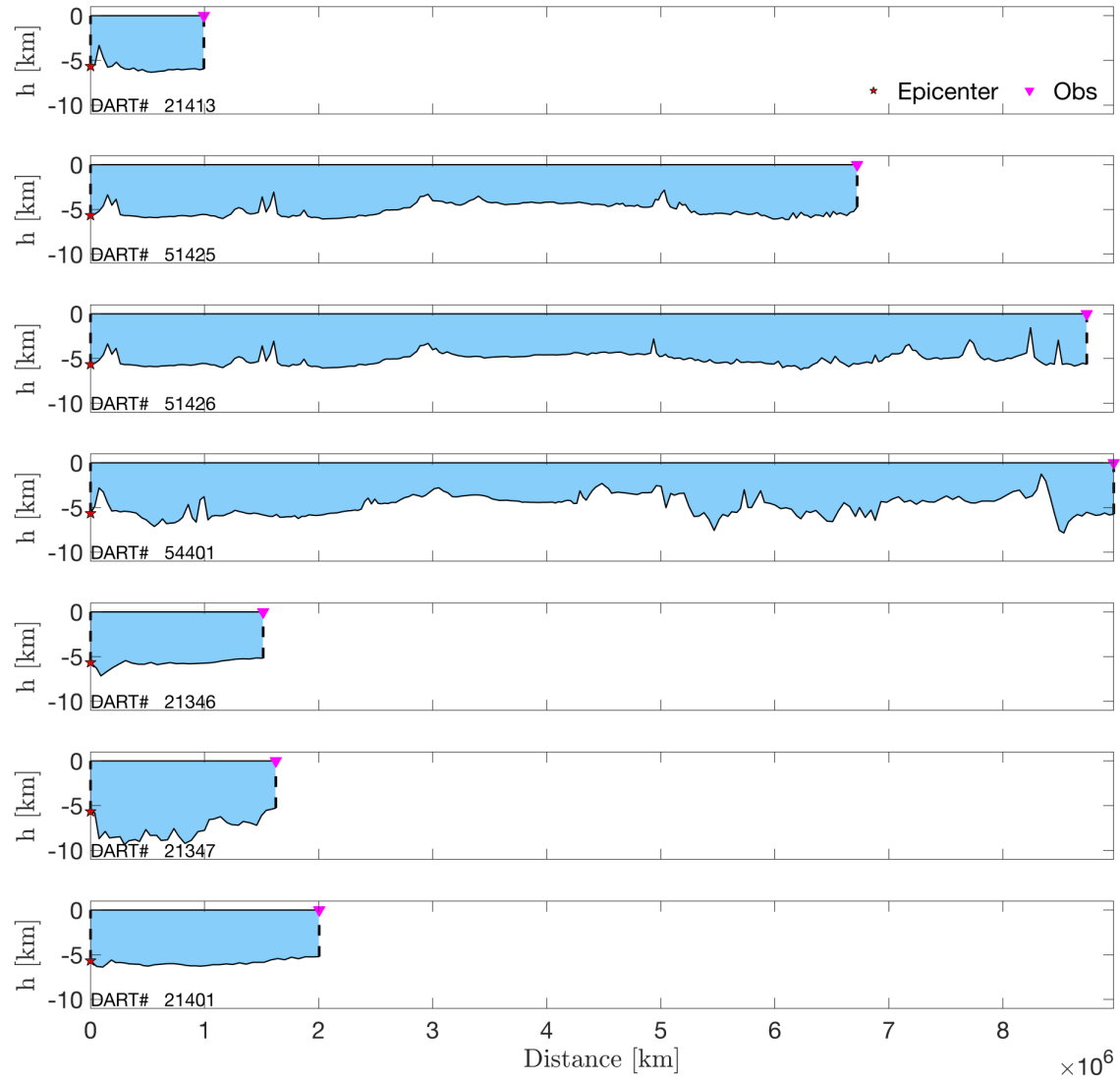


Figure 10- Transect along the shortest path between the epicenter and selected hotspots (DART stations) for 21st December 2010 (27.10N, 143.76E) earthquake.

REFERENCES

[1] Abdolali, A., Kadri, U. & J.T. Kirby, 2019, Effect of Water Compressibility, Sea-floor Elasticity, and Field Gravitational Potential on Tsunami Phase Speed, Scientific Reports, Nature, doi:10.1038/s41598-019-52475-0

Williams, B., Kadri, U., & Abdolali, A. (2021). Acoustic-gravity waves from multi-fault rupture. *Journal of Fluid Mechanics*, 915, A108. doi:10.1017/jfm.2021.101

Abdolali, A., Kadri, U., Parsons, W., & Kirby, J., 2018, On the propagation of acoustic-gravity waves under elastic ice sheets. *Journal of Fluid Mechanics*, 837, 640-656. doi:10.1017/jfm.2017.808 Cambridge Core Share access code 5A9FC1CA9902F823CDD1098A70442449

Gomez, B. and Kadri, U. 2021. Near real-time calculation of submarine fault properties using an inverse model of acoustic signals. *Applied Ocean Research* 109, article number: 102557. (10.1016/j.apor.2021.102557)

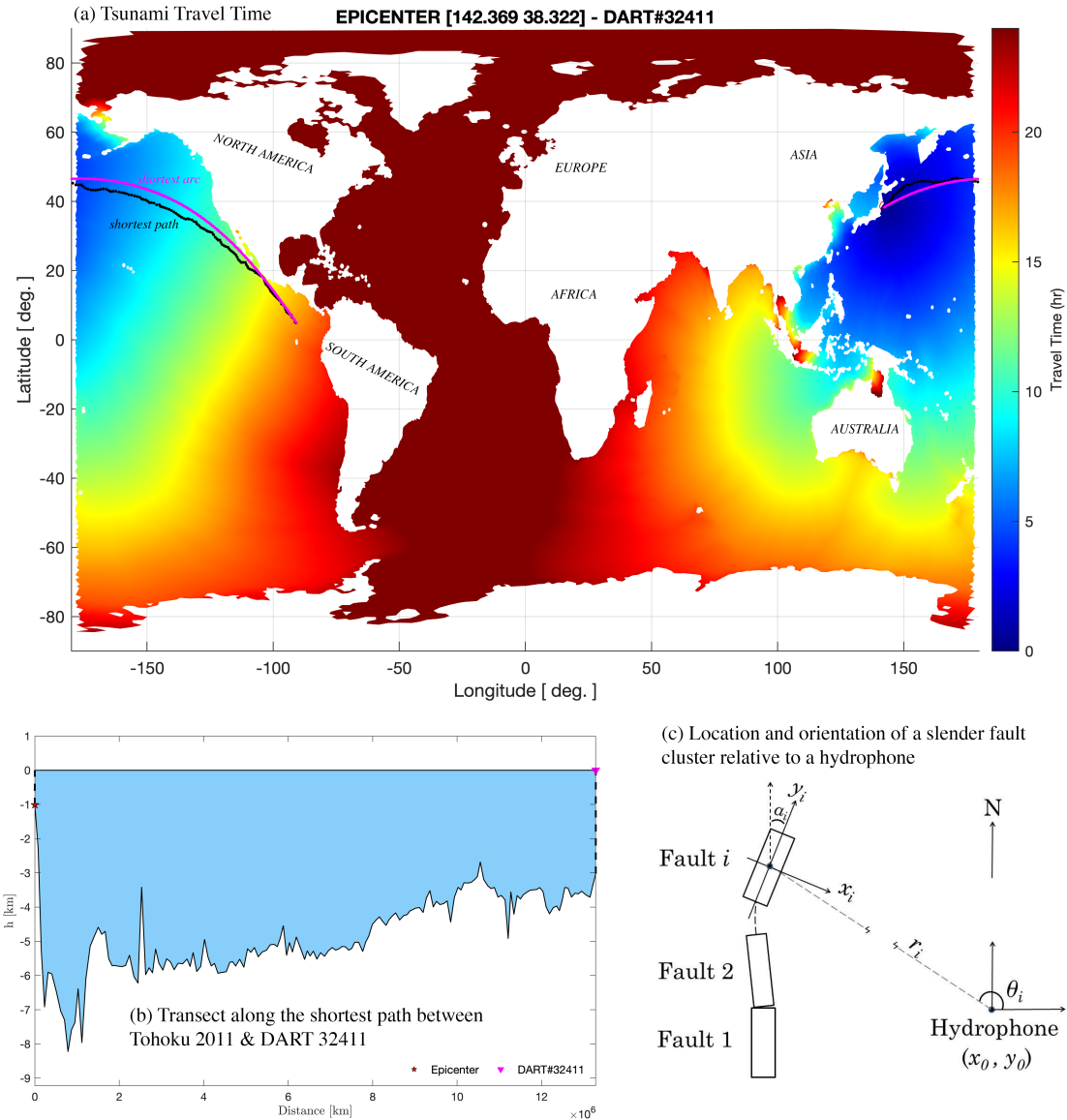
Gomez, B. and Kadri, U. 2021. Earthquake source characterization by machine learning algorithms applied to acoustic signals. *Scientific Reports*

ABSTRACT

The Dijkstra's algorithm is employed to find the shortest paths between the epicenter and all the wet nodes on a global triangular unstructured mesh using the phase speed of surface gravity waves and progressive acoustic modes. The phase speed estimator takes into account the simultaneous effects of the slight compressibility of water, sea-bed elasticity, and static compression of the ocean under gravity, leading to precise calculation of the arrival time [1]. Coupled to a mathematical solution for multi-fault rupture along the transect extracted from the shortest path between the source and destination is then employed to characterize the genesis of the tsunami [2]. The effectiveness of the aforementioned algorithms and distinct arrival time of different the tsunami and its precursor components (acoustic modes) at DART and deep ocean acoustic observations can be used for tsunami early warning systems.

[1] Abdolali, A., Kadri, U. & J.T. Kirby, 2019, Effect of Water Compressibility, Sea-floor Elasticity, and Field Gravitational Potential on Tsunami Phase Speed, *Scientific Reports, Nature*, doi:10.1038/s41598-019-52475-0 (<https://www.nature.com/articles/s41598-019-52475-0>)

[2] Williams, B., Kadri, U., & Abdolali, A. (2021). Acoustic-gravity waves from multi-fault rupture. *Journal of Fluid Mechanics*, 915, A108. doi:10.1017/jfm.2021.101 (<https://doi.org/10.1017/jfm.2021.101>)



(https://agu.confex.com/data/abstract/agu/fm21/5/4/Paper_941345_abstract_870770_0.png)

LINK TO A SURVEY

Enter your survey URL here

Submit

Delete